ChemComm

Accepted Manuscript

This article can be cited before page numbers have been issued, to do this please use: C. Yee, A. W. H. Ng and H. Y. Au-Yeung, *Chem. Commun.*, 2019, DOI: 10.1039/C9CC02263E.

ROYAL SOCIETY OF CHEMISTRY

rsc.li/chemcomm

ROYAL SOCIETY OF CHEMISTRY View Article Online
DOI: 10.1039/C9CC02263E

Journal Name

COMMUNICATION

Control over the macrocyclisation pathway and product topology in a copper-templated catenane synthesis

Received 00th January 20xx,
Accepted 00th January 20xx

DOI: 10.1039/x0xx00000x

www.rsc.org/

Chi-Chung Yee,[a] Antony Wing Hung Ng[a] and Ho Yu Au-Yeung[a,*]

We report here that the product topology in a copper-templated catenane synthesis can be controlled by favouring a particular macrocyclisation pathway, offering an additional strategy for improving the efficiency of catenane formation. A linear [4]catenane was obtained by non-covalently modifying a flexible building block that favours the intra-ligand cyclisation.

The unique mechanical, co-conformational and stereochemical properties of molecular links have recently emerged to different applications including molecular recognition,[1] sensing,[2] catalysis[3] and constructing molecular machines[4] which may not be achievable by their non-interlocked counterparts. Developing strategies to the efficient formation of interlocked macrocycles are therefore of central importance in the field. Although some simple catenanes (e.g. Hopf link) can now be considered to be straightforwardly accessible,[5] there are also reports of unsuccessful macrocycle interlocking despite of the use of some well-studied templates and ring-closing reactions. For example, it has been shown that the double macrocyclisation of two orthogonally arranged ligands on a Fe(II),[6] Co(III)[7] or Pd(II)[8] template gave no catenanes but only trivial macrocycles. Two independent works that both feature the ring-closing alkene metathesis of three pyridyl-2,6-diamine ligands coordinated on a lanthanide template also showed that a [3]catenane was obtained in one case,[9] whereas a mixture of a trefoil knot and a trivial macrocycle was resulted in another.[10] Few other examples that different topologies were obtained from the same template and ring-closing macrocyclisation have also been reported.[11] In all these cases, the subtle differences in the building block structures may have led to a different stability and/or orientation of the templated building blocks, which eventually resulted in different macrocyclisation pathways that affected their interlocking and the overall product topology.

Clearly, strategies for preorganisation and ring-closing are not sufficient for macrocycle interlocking and catenane formation. A further understanding on how the macrocycles are formed from the templated precursors is necessary for a predictable and reliable synthesis of molecular links. While structural modifications on the building blocks to optimise the stability and orientation of the preorganised precursors to improve the yields and topological selectivity is a viable strategy,[9-12] how the precursor intertwining and macrocycle interlocking are affected by the subtle and dynamic intermolecular interactions is not always obvious and clear.[13] On the other hand, strategies to control the macrocyclisation pathway could be a more straightforward and predictable strategy to achieve selectivity in product topology. By a good understanding of the structural features of the preorganised precursors and a judicious design of the complementary building blocks, some macrocyclisation pathways may be (dis)favoured to control the product topology. Here, we report the effect of covalent and non-covalent modification of the building block on the topological outcome in a copper-templated, imine-based catenane synthesis. By favouring the intra-ligand macrocyclisation, mechanically interlocked Hopf links and a linear [4]catenane were obtained in good yields.

Cu^+-bis(phenanthroline) was chosen as a model template because of its wide application in the synthesis of different interlocked molecules.[14] Due to the tetrahedral geometry of Cu^+, the two phenanthrolines are orthogonally arranged such that the intra-ligand macrocyclisation will give a Hopf link (Fig. 1c, green pathway), whereas the inter-ligand macrocyclisation will produce the topologically trivial molecular figure-eight (Fig. 1c, blue pathway). If the intra- or inter-ligand macrocyclisation can be promoted or suppressed by the use of an appropriate building block, formation of the interlocked rings could be controlled. X-ray crystallographic analysis of $[Cu(\mathbf{L1})_2][PF_6]$ showed the expected tetrahedral geometry. Stacking of the benzaldehyde and phenanthroline units are observed which may further stabilise the complex and direct the benzaldehydes to an orthogonal orientation. ^{1}H NMR of $[Cu(\mathbf{L1})_2]^+$ showed upfield shifts of the benzaldehyde protons

[a] Department of Chemistry, The University of Hong Kong, Pokfulam Road, Hong Kong, P. R. China. Email: hoyuay@hku.hk
Electronic Supplementary Information (ESI) available: [details of any supplementary information available should be included here]. See DOI: 10.1039/x0xx00000x

by ~0.6–1 ppm when compared with that of **L1**, suggesting the stacking interactions and orthogonal orientation are maintained in solutions (Fig. S33). The intra- and inter-ligand aldehyde distances are *ca.* 8.2 Å and 13.3–15.8 Å respectively. Ring-closing with a relatively short diamine could therefore favour the intra-ligand cyclisation to give a Hopf link, whereas a molecular figure-eight could be obtained by using a relatively long diamine. Of note, it is more common in literatures that only the yield of the (desired) interlocked molecules is reported, and the formation of other topology, especially the non-interlocked products, are rarely discussed. Detail analysis on building block structure and topological selectivity in a templated synthesis are therefore highly limited.[15]

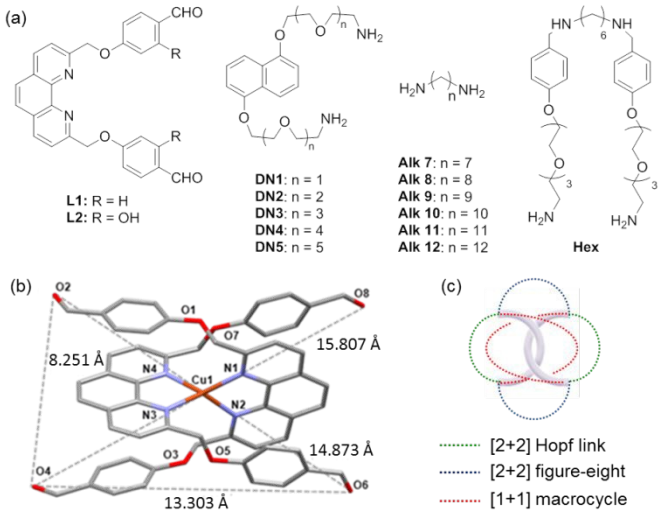

Fig. 1. (a) Chemical structures of the dialdehyde and diamine building blocks; (b) X-ray structure of $[Cu(\mathbf{L1})_2]^+$; and (c) possible products from different macrocyclisation pathways on a tetrahedral template.

The copper complex $[Cu(\mathbf{L1})_2]^+$ was condensed with a series of dioxynaphthalene-derived diamine of various lengths. The yield and topology of all the condensation products were analysed after reducing the dynamic imines to the corresponding amines. LCMS studies of a reaction mixture from $[Cu(\mathbf{L1})_2]^+$/**DN3** showed three major products: a [1+1] macrocycle **M3** in 14% yield and two isomeric [2+2] species (Fig. 2a). Topology of the two [2+2] products were characterised by MS^2, in which the major [2+2] product (**F3**, 58%) was suggested to be a trivial macrocycle because a sequential fragmentation with fragments larger than that of **M3** was observed (Fig. 2b). On the other hand, the minor [2+2] product (**H3**, 28%) was suggested to be a Hopf link due to its direct fragmentation to the [1+1] species (Fig. 2c). Notably, **F3** and **H3** are structural isomers (different bond connectivity) of different topology, and that **H3** and a pair of **M3** are topological isomers that differ only in their topology.[16]

H3 and **F3** were further characterised by ^{1}H NMR. As a figure-eight is chiral, H_d (*ca.* 4.4 ppm) in the Cu^+-coordinated, racemic **F3** are diastereotopic and were observed as a pair of doublet but remained as a singlet for the achiral **H3** (Fig. 3). In

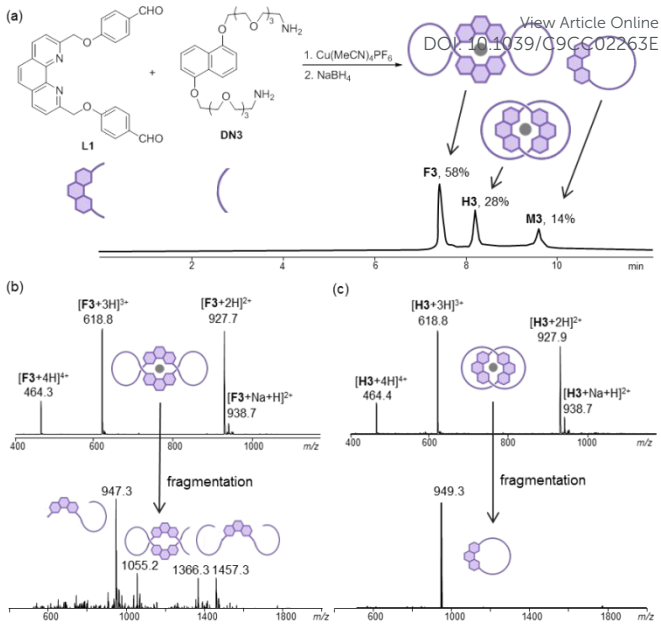

Fig. 2. (a) Cu^+-templated synthesis using **L1** and **DN3**, and the LC chromatogram of the product mixture. Also shown are the ESI-MS and MS^2 spectra of (b) **F3** and (c) **H3**.

addition, δ of the phenanthroline protons in **H3** are only slightly upfield shifted by ~0.1 ppm when compared with that of $[Cu(\mathbf{L1})_2]^+$, suggesting the Cu^+-phenanthroline core remains in a similar chemical environment. On the other hand, significant shifts were observed for the phenanthroline protons of **F3**, showing that the Cu^+-phenanthroline core is having a different conformation. In addition, NOE cross peaks between H_{DN} and H_{Ar} were observed in **F3** but not in **H3**, suggesting the aromatic units are in close proximity in the figure-eight but not the Hopf link (Fig. S43). Both the ^{1}H spectra showed one set of signals that suggest a symmetrical conformation for **H3** and **F3** on the NMR timescale.

Since the intra-ligand aldehyde distance is relatively shorter than of the inter-ligand, the use of a shorter diamine could favour the formation of the Hopf link. As expected, when the number of ethylene glycol units in **DN3** was decreased to 3 (**DN2**) and 2 (**DN1**), an increase in the yield of the Hopf link from 28% to 43% to 66% at the expense of the figure-eight was observed (Table 1). Ratio of the Hopf link to figure-eight increases from 0.48 to 1.06 to 3.14, with only a small variation in the yields of the [1+1] macrocycles. On the other hand, a further increase in the number of ethylene glycol units to 5 (**DN4**) and 6 (**DN5**) did not change significantly the ratio of the two products, and that the Hopf link to figure-eight ratio is kept at around 0.5. The plateauing of the Hopf link to figure-eight ratio could be due to the dynamic nature of the imine which results in a statistical ratio of the intra- and inter-ligand macrocyclisation. When the diamines are of a length such that the two [2+2] products are energetically similar, a 2:1 ratio of the inter- to intra-ligand macrocyclisation would be resulted upon the formation of the first imine on the tetrahedral template. In all cases, the [1+1] macrocycle was observed in 13–17% yield despite of the different length of the diamines. It

View Article Online
DOI: 10.1039/C9CC02675

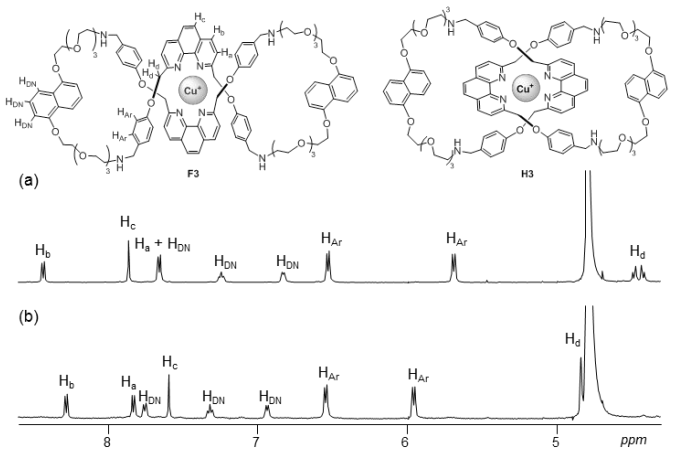

Fig. 3. Partial ^{1}H NMR (D_2O, 500 MHz, 298 K) of (a) **F3** and (b) **H3**.

is likely that these [1+1] macrocycles are formed from a non-preorganised ligand rather than a "back-side" macrocyclisation which is highly improbable (Fig. 1c, red). Based on these observations, it appears that the observed selectivity may be thermodynamic in origin, yet the need of imine reduction for the analysis may present additional complication in understanding the nature of the Hopf/figure-eight selectivity. Of note, **DN1** to **DN5** differ only by the number of the flexible ethylene glycol units with no obvious curvature, rigidity or moiety for additional interactions. With the same template and preorganised precursors being used, the difference in the Hopf link to figure-eight ratio is probably due to the different macrocyclisation pathway but not the stability or orientation of the preorganised precursors.[10,17]

Further demonstration of controlling the topological selectivity by favouring the intra-ligand macrocyclisation comes from another set of templated synthesis using $[Cu(\mathbf{L1})_2]^+$ and α,ω-alkyldiamines. Because of the significantly shorter length of the α,ω-alkyldiamines, the inter-ligand macrocyclisation could be further suppressed to favour Hopf link formation. Consistent with this proposal, LCMS analysis of mixtures from the reaction of $[Cu(\mathbf{L1})_2]^+$ and **Alkn** (n = 7–12) all showed the Hopf link as the only [2+2] product with no molecular figure-eight, indicating that the intra-ligand macrocyclisation is exclusively favoured (Table 1). The Hopf links **H6** to **H11** have been characterised by MS^2, ^{1}H and ^{13}C NMR and are consistent with their interlocked structures.

In addition to the use of diamine with a different covalent structure, effects of non-covalent modification of the building block were also investigated. Similar to **DN3**–**DN5**, condensation of **Hex** with $[Cu(\mathbf{L2})_2]^+$ gave a mixture with the non-interlocked **F12b** as the major product in 68% yield,[18] showing that the inter-ligand macrocyclisation is preferred. Interestingly, binding of CB[6] to the central hexanediamine unit that converted **Hex** to a [2]pseudorotaxane resulted in a change of the preferred macrocyclisation pathway to intra-ligand,[19] and the linear [4]catenane **H13** was obtained in 77% yield. A single set of temperature insensitive ^{1}H resonances was observed for **H13**, showing that the [4]catenane is

Table 1. Distribution of products of different topologies from templated syntheses using $[Cu(\mathbf{L1})_2]^+$ and $[Cu(\mathbf{L2})_2]^+$. Note that **H13**, **F13** and **M13** are respectively a [4]-, [3]- and [2]catenane.

diamine	[2+2] Hopf link	[2+2] Figure-eight	[1+1] Macrocycle	intra: inter
DN1*	**H1b**, 66%	**F1b**, 21%	**M1**, 13%	3.14
DN2	**H2**, 43%	**F2**, 40%	**M2**, 17%	1.06
DN3	**H3**, 28%	**F3**, 58%	**M3**, 14%	0.48
DN4	**H4**, 28%	**F4**, 56%	**M4**, 16%	0.50
DN5	**H5**, 29%	**F5**, 56%	**M5**, 15%	0.52
Alk7	**H6**, 82%	/	**M6**, 18%	/
Alk8	**H7**, 86%	/	**M7**, 14%	/
Alk9	**H8**, 84%	/	**M8**, 16%	/
Alk10	**H9**, 82%	/	**M9**, 18%	/
Alk11	**H10**, 82%	/	**M10**, 18%	/
Alk12	**H11**, 83%	/	**M11**, 17%	/
Hex*	**H12b**, 20%	**F12b**, 68%	**M12**, 11%	0.29
Hex·CB[6]	**H13**, 77%	**F13**, 8%	**M13**, 15%	8.56

* Determined after demetallation because of peak overlapping.

adopting a relatively rigid conformation in solution (Fig. S74). The comparable δ values for the aromatic protons of **H13** to that of **H3**, and the observed singlet of H_d (at ~4.8 ppm at 358 K) are also consistent with the linear [4]catenane topology. On the other hand, inter-ligand macrocyclisation using **Hex**·CB[6] gave the [3]catenane **F13** with a twisted central macrocycle in a figure-eight conformation in only 8% yield, corresponding to a switch in the product selectivity by about 30 times (Fig. 4). The ^{1}H spectrum of **F13** consists of only broad signals that are sharpened slightly at higher temperature, suggesting that **F13** is conformationally more flexible than **H13**. Of note, linear [n]catenanes are often obtained in low yields and are relatively rare when compared to radial counterparts.[5a,20] The present efficient synthesis of **H13** could be implicated in the synthesis of other high-order catenanes that are to be realised.

In summary, control over the product topology in a templated synthesis using either covalent or non-covalent strategies is demonstrated, and a rare linear [4]catenane was obtained in one simple step in 77% yield. In addition to conventional optimisation of the non-obvious and subtle stability/orientation of the preorganised precursors and limiting possible macrocyclisation pathways, the present results offer straightforward and alternative strategies for the simple and effective control over the product topology in a templated synthesis which is central to both the fundamental chemistry and new applications of molecular links and knots.

This work is supported by the Croucher Foundation and a grant from the Research Grants Council of the Hong Kong SAR, China (HKU 27300014). C.-C. Y. and A. W. H. N. are recipients of the Postgraduate Scholarship from The University of Hong

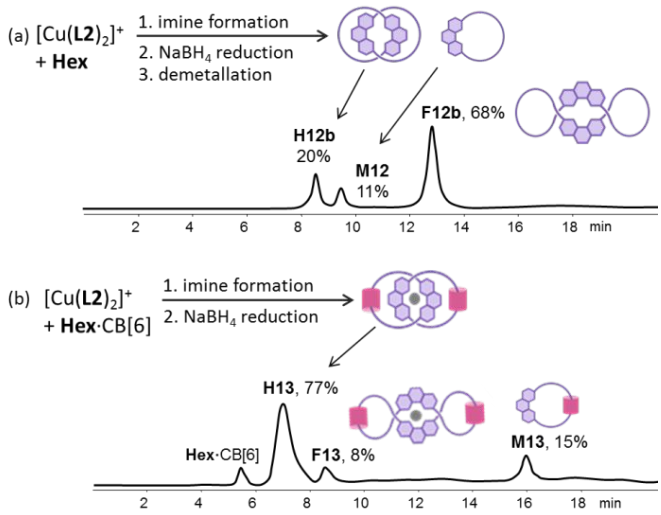

Fig. 4. Supramolecular binding to CB[6] switched the preferred macrocyclisation from (a) inter-ligand to (b) intra-ligand. A slight excess (~5%) of **Hex**·CB[6] was used to ensure a complete imine formation.

Kong. We acknowledge UGC funding administered by The University of Hong Kong for support of the Electrospray Ionisation Quadrupole Time-of-Flight Mass Spectrometry Facilities under the support for Interdisciplinary Research in Chemical Science.

Conflict of interest

There are no conflicts to declare.

Notes and references

1 (a) M. J. Langton and P. D. Beer, *Chem. Commun.* 2014, **550**, 8124; (b) R. Mitra, M. Thiele, F. Octa-Smolin, M. C. Letzel and J. Niemyer, *Chem. Commun.* 2016, **52**, 5977.
2 (a) M. J. Langton and P. D. Beer, *Acc. Chem. Res*. 2014, **47**, 1935; (b) T. A. Barendt, L. Ferreira, I. Marques, V. Felix and P. D. Beer, *J. Am. Chem. Soc*. 2017, **139**, 9026.
3 N. Pairault and J. Niemeyer, *Synlett* 2018, **29**, 689.
4 (a) J. V. Hernandez, E. R. Kay and D. A. Leigh, *Science* 2004, **306**, 1532; (b) J. M. Spruell, W. F. Paxton, J. Olsen, D. Benitez, E. Tkatchouk, C. L. Stern, A. Trabolsi, D. C. Friedman, W. A. Goddard III and J. F. Stoddart, *J. Am. Chem. Soc.* 2009, **131**, 11571; (c) D. A. Leigh, J. K. Y. Wong, F. Dehez and F. Zerbetto, *Nature* 2003, **424**, 174.
5 (a) C. J. Burns and J. F. Stoddart, *The Nature of The Mechanical Bond: From Molecules to Machines*, John Wiley & Sons, New Jersey, 2017; (b) E. R. Kay, D. A. Leigh and F. Zerbetto, *Angew. Chem., Int. Ed.* 2007, **46**, 72; (c) G. Gil-Ramírez, D. A. Leigh and A. J. Stephens, *Angew. Chem., Int. Ed.* 2015, **54**, 6110; (d) M. Denis and S. M. Goldup *Nat. Chem. Rev.* 2017, **1**, 61; (e) N. H. Evans and P. D. Beer, *Chem. Soc. Rev.* 2014, **43**, 4658; (f) H. Y. Au-Yeung, C.-C. Yee, A. W. H. Ng and K. Hu, *Inorg. Chem.* 2018, **57**, 3475; (g) J. E. Beves, B. A. Blight, C. J. Campbell, D. A. Leigh and R. T. McBurney, *Angew. Chem., Int. Ed.* 2011, **50**, 9260; (h) J. D. Crowley, S. M. Goldup, A.-L. Lee, D. A. Leigh and R. T. McBurney, *Chem. Soc. Rev.* 2009, **38**, 1530.
6 N. Belfrekh, C. Dietrich-Buchecker and J.-P. Sauvage, *Inorg. Chem.* 2000, **39**, 5169.
7 D. A. Leigh, P. J. Lusby, R. T. Mcburney, A. Morelli, A. M. Z. Slawin, A. R. Thomson and D. B. Walker, *J. Am. Chem. Soc.* 2009, **131**, 3762.
8 A.-M. L. Fuller, D. A. Leigh, P. J. Lusby, A. M. Z. Slawin and D. B. Walker, *J. Am. Chem. Soc.* 2005, **127**, 12612.
9 C. Lincheneau, B. Jean-Denis and T. Gunnlaugsson. *Chem. Commun.* 2014, **50**, 2857.
10 J.-F. Ayme, G. Gil-Ramírez, D. A. Leigh, J.-F. Lemmonier, A. Markevicius, C. A. Muryn and G. Zhang, *J. Am. Chem. Soc.* 2014, **136**, 13142.
11 (a) J. E. Beves, J. J. Danon, D. A. Leigh, J.-F. Lemonnier and I. J. Vitorica-Yrezabal, *Angew. Chem., Int. Ed.* 2015, **54**, 7555; (b) J. J. Danon, D. A. Leigh, S. Pisano, A. Valero and I. J. Vitorica-Yrezabal, *Angew. Chem., Int. Ed.* 2018, **130**, 14029.
12 (a) G. Zhang, G. Gil-Ramirez, A. Markevicius, C. Browne, I. J. Vitorica-Yrezabal and D. A. Leigh, *J. Am. Chem. Soc.* 2015, **137**, 10437; (b) L. Zhang, A. J. Stephens, A. L. Nussbaumer, J.-F. Lemonnier, P. Jurček, I. J. Vitorica-Yrezabal and D. A. Leigh, *Nat. Chem.* 2018, **10**, 1083; (c) J. J. Danon, A. Krüger, D. A. Leigh, J.-F. Lemonnier, A. J. Stephens, I. J. Vitorica-Yrezabal and S. L. Woltering, *Science* 2017, **355,** 159.
13 (a) K. Caprice, M. Pupier, A. Kruve, C. Schalley and F. B. L. Cougnon *Chem. Sci.* 2018, **9**, 1317; (b) F. B. L. Cougnon, K. Caprice, M. Pupier, A. Bauza and A. Frontera *J. Am. Chem. Soc.* 2018, **140**, 12422; (c) C.-Y. Wang, G. Wu, T. Jiao, L. Shen, G. Ma, Y. Pan and H. Li *Chem. Commun.* 2018, **54**, 5106; (d) M. E. Dehkordi, V. Luxami and G. D. Pantoş *J. Org. Chem.* 2018, **83**, 11654.
14 (a) S. Durot, F. Reviriego and J.-P. Sauvage, *Dalton Trans.* 2010, **39**, 10557; (b) J.-P. Sauvage, *Acc. Chem. Res.* 1990, **23**, 319; (b) C. O. Dietrich-Buchecker and J.-P. Sauvage, *Chem. Rev.* 1987, **87**, 795; (d) K. Wang, C.-C. Yee and H. Y. Au-Yeung, *Chem. Sci.* 2016, **7** 3787; (e) R. Hayashi, P. Slavik, Y. Mutoh, T. Kasama and S. Saito, *J. Org. Chem.* 2016, **81**, 1175; (f) J. D. Megiatto Jr. and D. I. Schuster *J. Am. Chem. Soc.* 2008, **130**, 12872; (g) J. A. Berrocal, M. M. L. Nieuwenhuizen, L. Mandolini, E. W. Meijer and S. D. Stefano, *Org. Biomol. Chem.* 2014, **12**, 6167; (h) K.-L. Tong, C.-C. Yee, Y. C. Tse and H. Y. Au-Yeung, *Inorg. Chem. Front.* 2016, **3**, 348.
15 C. O. Dietrich-Buchecker, A. Edel, J. P. Kintzinger and J.-P. Sauvage, *Tetrahedron* 1987, **43**, 333.
16 (a) D. M. Walba, *Tetrahedron* 1985, **41**, 3161; (b) G. A. Breault, C. A. Hunter and P. C. Mayers, *Tetrahedron* 1999, **55**, 5265.
17 J. R. Price, J. K. Clegg, R. R. Fenton, L. F. Lindoy, J. C. Mcmurtrie, G. V. Meehan, A. Parkin, D. Perkins and P. Turner, *Aus. J. Chem.* 2009, **62**, 1014.
18 Imine formation is facilitated by the ortho-OH group in **L2**: M.-S. Seo, S. Jang, H. Jung and H. Kim, *J. Org. Chem.* 2018, **83**, 14300.
19 (a) W. L. Mock and N. Y. Shih, *J. Org. Chem.* 1986, **51**, 4440; (b) W. L. Mock and N. Y. Shih, *J. Am. Chem. Soc.* 1988, **110**, 4706.
20 (a) Q. Wu, P. M. Rauscher, X. Lang, R. J. Wojtecki, J. J. de Pablo, M. J. A. Hore and S. J. Rowan, *Science* 2017, **358**, 1434; (b) H. Iwamoto, S. Tafuku, Y. Sato, W. Takizawa, W. Kitagiri, E. Tayama, E. Hasegawa, Y. Fukazawa and T. Haino, *Chem. Commun.* 2015, **52**, 319; (c) C.-H. Lu, X.-J. Qi, A. Cecconello, S.-S. Jester, M. Famulok and I. Willner, *Angew. Chem., Int. Ed.* 2014, **53**, 7499; (d) F. Schwanke, O. Safarowsky, C. Heim, G. Silva and F. Vögtle, *Helv. Chim. Acta* 2000, **83**, 3279; (e) D. B. Amabilino, P. R. Ashton, V. Balzani, S. E. Boyd, A. Credi, J. Y. Lee, S. Menzer, J. F. Stoddart, M. Venturi and D. J. Williams, *J. Am. Chem. Soc.* 1998, **120**, 4295.

View Article Online
DOI: 10.1039/C9CC02263E

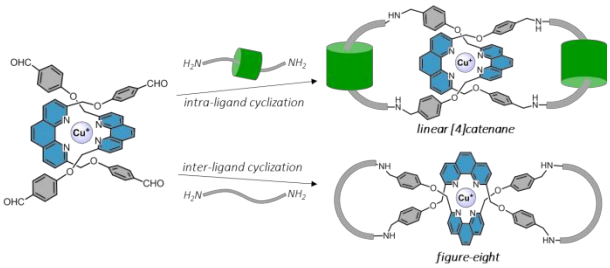

Strategies to control building block intertwining and the efficient assembly of a linear [4]catenane are presented.